

Accurate Models for Spiral Resonators

Ellstein, D.; Wang, B.; Teo, K.H.

TR2012-089 October 2012

Abstract

Analytically-based circuit models for two types of spiral resonators, a single layer and a double layer spiral, are given. The models are suitable for various spiral and wire crosssectional shapes. The double layer spiral is composed of two identical spirals of opposite winding in which the inner or outer leads may or may not be connected, such as through a via. For both types, the model can account for the effect of a dielectric slab. The advantage of these models to previous circuit models is shown through their comparison to experimental measurements and numerical simulations.

European Radar Conference (EuRAD) 2012

This work may not be copied or reproduced in whole or in part for any commercial purpose. Permission to copy in whole or in part without payment of fee is granted for nonprofit educational and research purposes provided that all such whole or partial copies include the following: a notice that such copying is by permission of Mitsubishi Electric Research Laboratories, Inc.; an acknowledgment of the authors and individual contributions to the work; and all applicable portions of the copyright notice. Copying, reproduction, or republishing for any other purpose shall require a license with payment of fee to Mitsubishi Electric Research Laboratories, Inc. All rights reserved.

Accurate Models for Spiral Resonators

David Ellstein, Bingnan Wang, and Koon Hoo Teo

Mitsubishi Electric Research Laboratories, 201 Broadway, Cambridge, MA 02139

Abstract — Analytically-based circuit models for two types of spiral resonators, a single layer and a double layer spiral, are given. The models are suitable for various spiral and wire cross-sectional shapes. The double layer spiral is composed of two identical spirals of opposite winding in which the inner or outer leads may or may not be connected, such as through a via. For both types, the model can account for the effect of a dielectric slab. The advantage of these models to previous circuit models is shown through their comparison to experimental measurements and numerical simulations.

Index Terms — Circuit analysis, circuit topology, EM models, resonators, spirals

I. INTRODUCTION

Spiral resonators (SRs) have numerous applications. These include constituting metamaterials [1], filtering [2], and working as a telemetric force sensor [3]. Thus an accurate model of SRs is important. This paper focuses on an improved circuit model of a single layer spiral (SLS) and a double layer spiral (DLS). The two identical spirals forming a DLS are oppositely wound and may be connected by a conductor, such as a via.

Previous circuit models of an SLS (such as for an Archimedes' or square spiral) use the same circuit topology, a tank circuit model [1] [2]. Although the expressions used for calculating the component values of the circuit may differ between the models, all the models share the same technique in analyzing the SR into a tank circuit model. The inductance of the tank circuit model is calculated by assuming the current throughout the spiral is uniform. The capacitance of the tank circuit is assumed to be the parallel equivalent of the capacitances corresponding to each pair of adjacent loops. The tank circuit model presumes that the SR has only a single resonant frequency. Thus it may not be used to get insight into the electromagnetic properties of the single layer spiral over a large frequency span.

Previous circuit models of a DLS (such as formed by Archimedes' or square spirals) vary greatly in their topology [3][4]. The models are generally focused on their application of the DLS as an inductor instead of an SR [3]. An exception is the SR used as a telemetric force sensor [4]. Like the SLS model, these models do not predict the multiple resonant frequencies of the SRs and cannot give insight into the actual current distribution throughout the spiral.

In this paper analytically-based circuit models for a SLS and a DLS are given. These models can give more insight into the electromagnetic properties of SRs. In addition, the results of the circuit models are compared to experimental results and simulations using the commercial software Sonnet [5]. Sonnet

is a 3D planar electromagnetic simulator, based on the Method of Moments [5].

II. CIRCUIT MODELS OF SPIRAL RESONATORS

A. Development of Circuit Topology

The circuit models of both types of SRs are developed by modeling each loop as an isolated entity, a unit, and then modeling its connections and electromagnetic coupling with the other loops. The unit is composed of the series combination of a resistor and an inductor that models the intrinsic resistance and self-inductance of the corresponding loop. These units are then electrically connected in the sequence in which the physical loops of the spiral(s) are connected.

The next step in the development of the circuit model is the inclusion of the capacitive and inductive coupling between loops. The capacitance between nearby loops of the spiral(s) is modeled by adding capacitors connecting the respective loops. In order to better reflect the distributed nature of the capacitance, two capacitors, each half the total capacitance between the loops, are connected between the respective units. The capacitors connect the ends of the loops (one end from each loop) that are nearest. The inductive coupling between loops sharing significant magnetic flux is modeled as mutual inductance between the inductors of the corresponding units. This mutual inductance is not explicitly shown in the circuit models.

Using this methodology the general circuit model of an SLS and DLS was made. Fig. 1 and Fig. 2 contain a picture of a physical SR and its corresponding circuit model for an SLS and a DLS respectively. The SLS model only models the capacitance between adjacent loops. The DLS model only models the capacitance between opposing loops. Both models model the mutual inductance between all loops. A conductive connection between the leads, such as a via, is modeled by shorting the leads in the circuit model.

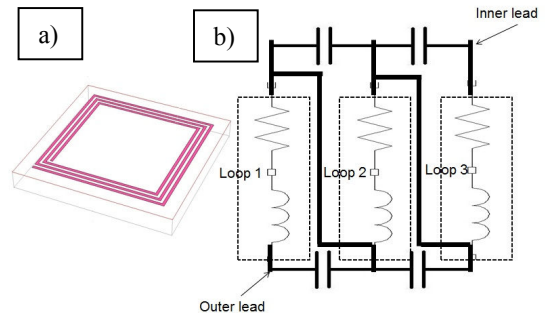


Fig. 1. A single layer spiral: a) physical structure and b) circuit model.

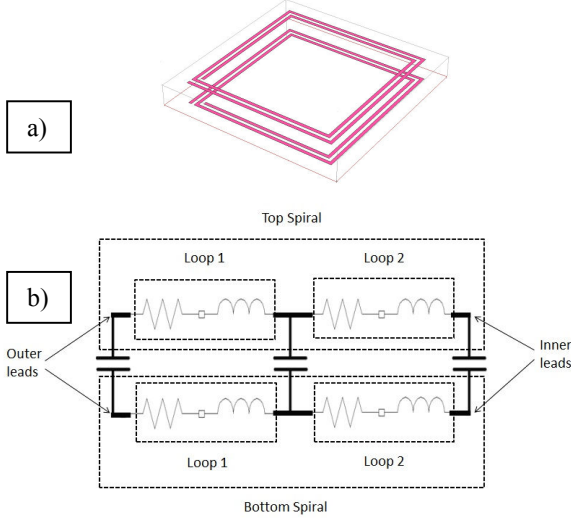


Fig. 2. A double layer spiral: a) physical structure and b) circuit model.

B. Analytical Calculation of Component Values

The exact analytical expressions used for calculating the component values depend on the shape of the spiral(s) forming the SR. However, independent of the shape there are some general methods that can be used to find the component values. In addition, it is helpful to approximate the shape of the loop such that the existing, simple analytical models for calculating the component values can be used. For example, the loops of an Archimedes' or square spiral may be well approximated by circles or squares respectively.

The values of the resistance of a loop are analytically calculated. The conductive resistance can be modeled using a skin-effect model, where the current density is largest near the surface. For a metallic wire with rectangular cross section, with width w and thickness at least 3 times larger than skin depth, the conductive resistance is simplified as

$$R_{cond} = \frac{l}{\sigma_c \delta w} = \frac{1}{w} \sqrt{\frac{\pi f \mu_c}{\sigma_c}}, \quad (1)$$

where σ_c is the conductance of the metal, f is excitation frequency, μ_c is permeability of metal, and δ is skin depth. Resistance of wire with different cross section can be calculated similarly.

The self-inductance of a loop may be found by using the relationship that the self-inductance is the magnetic flux through the loop divided by the uniform current magnitude assumed in the loop. For a circular loop with diameter D and rectangular cross section with width w , the inductance is approximated by the Equation (2) assuming w is much smaller than D .

$$L \approx \mu_0 \cdot \frac{D}{2} \cdot \left(\ln \left(\frac{8 \cdot D}{w} \right) - 2 \right) \quad (2)$$

Similarly for a square loop with side length D , the inductance is approximately by Equation (3).

$$L \approx \frac{2\mu_0}{\pi} D \left(\sinh^{-1} \left(\frac{2D}{w} \right) - 1 \right) \quad (3)$$

The interactions between loops are modeled as inductive coupling and capacitive coupling, and also calculated analytically.

The mutual inductance is the ratio of the magnetic flux through one of the loops due to the other loop divided by the uniform current magnitude assumed flowing in the other loop. Simple analytical models for concentric circular loops and for concentric square loops can be derived analytically. The mutual inductance between two concentric loops of loop radius and conductor width r_1 and w_1 , and r_2 and w_2 , separated by a distance h is given in Equations (3) through (6). The expression depends on the complete elliptic integrals of the first and second kind, $K[\kappa]$ and $E[\kappa]$, respectively.

$$M_{12} = \mu \sqrt{(r_1 - w_1) \cdot \left(r_2 - \frac{w_2}{2} \right)} \cdot \left[\left(\frac{2}{\kappa} - \kappa \right) K[\kappa] - \frac{2}{\kappa} E[\kappa] \right] \quad (4)$$

$$\kappa \equiv \frac{\sqrt{4 \cdot (r_1 - w_1) \cdot \left(r_2 - \frac{w_2}{2} \right)}}{\sqrt{h^2 + \left(r_1 + r_2 - w_1 - \frac{w_2}{2} \right)^2}} \quad (5)$$

$$K[\kappa] \equiv \int_0^{\pi/2} \frac{d\varphi}{\sqrt{1 - \kappa^2 \sin^2(\varphi)}} \quad (6)$$

$$E[\kappa] \equiv \int_0^{\pi/2} \sqrt{1 - \kappa^2 \sin^2(\varphi)} d\varphi \quad (7)$$

The analytical expression for the capacitance between adjacent loops is dependent on the location of the dielectric and the cross-sectional shape of the conductor. For two traces (rectangular cross section) on a dielectric (printed circuit board in many cases), or separated by a dielectric, good approximations exist based on the mathematical technique known as conformal mapping [6, 7]. Consider two parallel metallic traces with length l , trace width w , and spacing s on a dielectric substrate with the dielectric constant ϵ_r , and thickness of the slab h , the capacitance C is calculated by Equations (8) through (14). The elliptic integral $K[\kappa]$ is defined in Equation (6).

$$C = \epsilon_0 \epsilon_{eff} l \frac{K[k'_0]}{K[k_0]} \quad (8)$$

$$\epsilon_{eff} = 1 + (\epsilon_r - 1)q \quad (9)$$

$$q = \frac{1}{2} \frac{K[k']K[k_0]}{K[k]K[k_0']} \quad (10)$$

$$k = \frac{\tanh\left(\frac{\pi s}{4h}\right)}{\tanh\left(\frac{\pi(2w+s)}{4h}\right)} \quad (11)$$

$$k' = \sqrt{1 - k^2} \quad (12)$$

$$k_0 = \frac{s}{2w + s} \quad (13)$$

$$k_0' = \sqrt{1 - k_0^2} \quad (14)$$

Based on the above equations, the equivalent circuit component values can be calculated depending on the geometry, layout and material of the spiral. Once the circuit component values are obtained, they can be used to fit into the circuit topology developed in previous section for resonant frequency calculations.

III. RESONANT FREQUENCY

Initial validity tests of the proposed circuit models were done through comparing their prediction of the lowest resonant frequency of various SRs with experimental and simulated results. There are multiple ways of defining a resonant frequency. In the research for this paper a resonant frequency of an SR was found in a similar manner for the circuit model, simulation and through experimentation. Specifically, electromagnetic energy was coupled into the SR through magnetic induction by a loop antenna. In this paper the resonant frequency is defined as a local minimum in the S_{11} magnitude at the input to the loop antenna [8]. In Fig. 3 a drawing of the system for exciting and measuring the SR is given, along with a typical measurement of the S_{11} magnitude in decibels versus frequency.

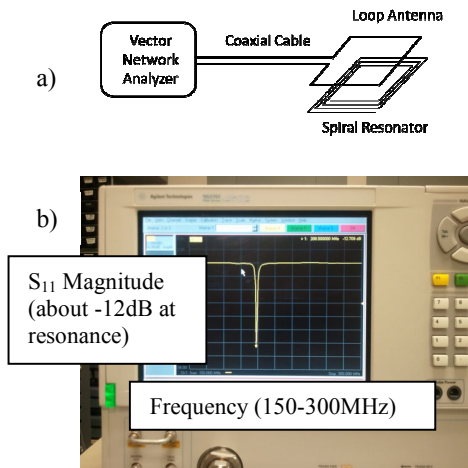


Fig. 3. Resonant frequency measurement: a) system setup and b) result.

In order to predict the resonant frequency using the circuit model approach, a circuit model of the loop antenna, along with its inductive coupling with the loops of the SR was added to the circuit model of the SR. The loop antenna, powered by an ideal voltage source, was modeled as the series combination of an inductor and a resistor. The inductive coupling between the loop antenna and the SR is modeled by a mutual inductance term for each loop of the SR. The goal of this circuit analysis is to find the input impedance seen by a voltage source. By assuming a voltage for the voltage source, the current in each path of the circuit model can be calculated. The input impedance seen by the voltage source is the ratio of the assumed voltage to the current coming out of the voltage source. With this complex value, which is a function of the frequency, the S_{11} value describing the input to the system (the loop antenna coupled to the spiral) may be easily calculated and plotted as a function of frequency. The resonant frequencies of the SRs were found experimentally by measuring the S_{11} magnitude using a vector network analyzer (VNA). Port 1 of the VNA was attached to the leads of the loop antenna. The resonant frequencies of the SRs were found through the simulation of the S_{11} magnitude of the system in Sonnet. Using the computer aided design (CAD) interface in Sonnet, the geometry and material properties of the system (SR and loop antenna) were inputted.

IV. RESULTS

Multiple SLSs and DLSs were manufactured on printed circuit boards (PCBs). All of them had the properties listed in Table I but they varied in the number of loop that composed them. In addition, DLSs were manufactured with and without a via connecting their respective inner leads. Fig. 4 show some manufactured samples for each type of spirals.

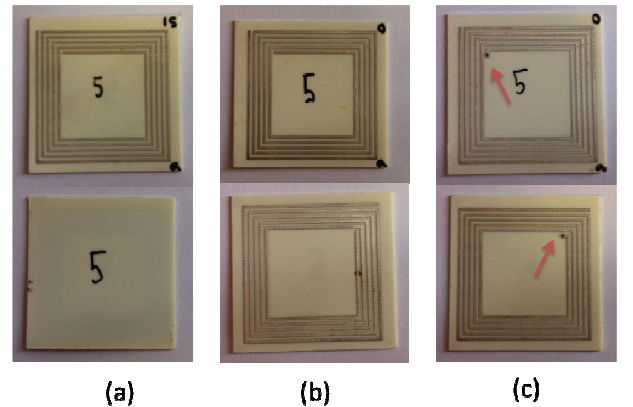


Fig. 4. Pictures of manufactured samples of (a) single layer spiral, (b) double layer spiral without via, and (c) double layer spiral with via.

via (pointed to by the red arrows). Top and bottom pictures show the two sides of each spiral.

The loop antenna has the same properties as the SRs except that it has a trace width of 1mm and its outermost dimensions are 35mm x 35mm. The loop antenna was placed 10mm above the SR. The resonant frequency of the SRs were predicted and experimentally found. The results of the presented circuit models, experimental results, and simulations in Sonnet are shown graphically in Fig. 5a and 5b for the SLS and DLS respectively.

The circuit model for the SLS shows the general trend of the resonant frequency as a function of the number of loops. However, as the number of loops increases, its error increases. The model may be improved by including the capacitance between non-adjacent loops. The DLS model with and without a via is much more accurate than the SLS model.

The DLS model agrees nicely with numerical and experimental results over a large range in the number of loops, for both types of spirals with or without via connections between two layers. The small difference between circuit model and rigorous numerical results is due to the approximations used for both the analytical calculations of the circuit component values and the circuit model itself.

TABLE I
GEOMETRIC AND MATERIAL PROPERTIES OF SRs

Trace Material	Copper
Trace Width	0.5mm
Trace Spacing	0.5mm
Trace Thickness	35 μ m
Outermost Dimensions	25mm x 25mm
Board Dielectric Constant	3.48
Board Dissipation Factor	0.004
Board Thickness	0.5mm

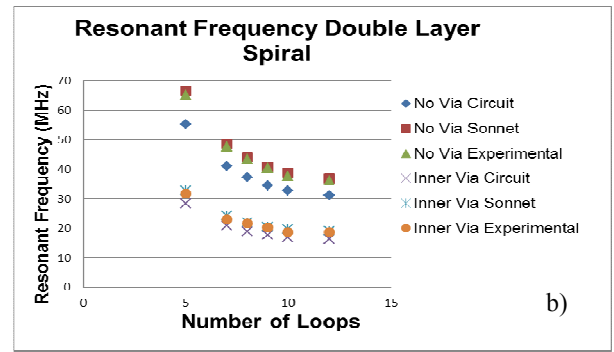
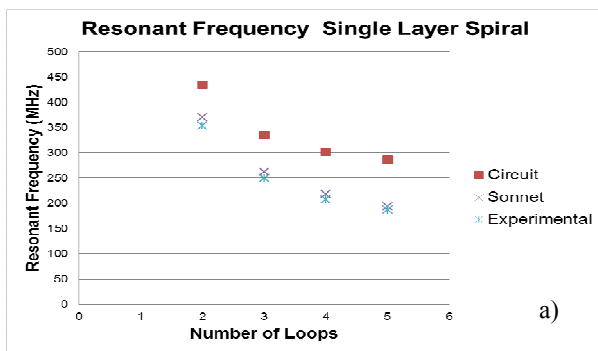


Fig. 5. Comparison of lowest resonant frequency prediction of the a) SLS and the b) DLS (with and without an inner via).

V. CONCLUSION

A novel circuit model of a single layer and a double layer spiral were presented. In addition, analytical expressions for calculating the circuit component values were described. These models can better reflect the standing wave current distribution in the spiral(s) than previous models. In addition, the models can predict some of the higher resonant frequencies of the SRs. Lastly, they can be analyzed very quickly relative to numerical simulations of SRs. The initial tests described above show that these models have promise in the accurate modeling of SRs composed of a range of loops.

REFERENCES

- [1] O. Isik and K. P. Esselle, "Design of Archimedean spiral resonators and bandwidth enhancement in filter applications," *2nd International Congress on Advanced Electromagnetic Materials in Microwaves and Optics, Pamplona, Spain, 2008*, pp. 341-343.
- [2] S. Nemer, et al., "Modelling Resonance Frequencies of a Multi-Turn Spiral for Metamaterial Applications," *Progress In Electromagnetics Research C*, vol. 20, pp. 31-42, 2011.
- [3] C. C. Collins, "Miniature Passive Pressure Transensor for Implanting in the Eye," *IEEE Trans. Biomed. Eng.*, vol. 14, April 1967.
- [4] J. N. Burghartz, et al., "Multilevel-Spiral Inductors Using VLSI Interconnect Technology," *IEEE Electron Device Lett.*, vol. 17, Sept. 1996.
- [5] Sonnet. (2011, Dec. 5). Sonnet Suites [Online]. Available: <http://www.sonnetsoftware.com/products/sonnet-suites/>
- [6] S. Gevorgian, et al., "Basic parameters of Coplanar-Strip Waveguides on Multilayer Dielectric/Semiconductor Substrates, Part 1: High Permittivity Superstrates," *IEEE Microwave*, vol. 4, pp. 60-70, June 2003.
- [7] H. B. Palmer, "The Capacitance of a Parallel-Plate Capacitor by the Schwartz-Christoffel Transformation," *Trans. of the American Institute of Electrical Engineers*, vol. 56, no. 3, pp. 363-366, 1937.
- [8] D. M. Pozar, "The Scattering Matrix," in *Microwave Engineering*, 2nd ed. New York: John Wiley & Sons, 1998, ch. 4, sec. 3, pp. 196-206.